A Nanobiomimetic Neural Memcapacitor Serves as a Voltage Sensor and an Amperometry Sensor for Reagent-less Direct Detection of Sub pM Soluble Amyloid-β

S-H. Duh[1], J. Thornton[2], P.T. Kissinger[3] and E. T. Chen[4*]

[1]University of Maryland Medical System, 22 South Greene St, Baltimore, MD 21201, USA
[2] Bruker Nano, 19 Fortune Dr., Billerica, MA 01821, USA
[3]Department of Chemistry, Purdue University, West Lafayette, IN 47906, USA
[4]Advanced Biomimetic Sensors, Inc., 11140 Rockville Pike, Suite 440, Unit 422, Rockville, MD 20852, USA, *ellenchen@nanobiomimeticsensors.com*

ABSTRACT

Challenges of quantitative detection of Amyloid-beta (Aβ) in Alzheimer's brains are paramount, such as the instability of soluble $A\beta_{1-42}$ in biological specimens, the interferences among proteins and the time consuming assays. A memcapacitor device was developed with nanostructured biomimetic acetylcholinesterase (ACHE) gorge membrane on gold chips, served as an artificial normal brain motif, has detected voltage and current changes in sub pM Aβ under conditions of free from antibodies and tracers using spiked NIST SRM 965A human serum, based on the characteristics of memcapacitor/memristor. The results of Detection of Limits (DOL) are $5.0x10^{-11}M/cm^2$ vs. $7.0x10^{-13}M/cm^3$ over the linear range at 0.04-151 nM vs. 3.8-471 nM, for the chronoamperometry (CA) and double step chronopotentiometry (DSCPO) methods, respectively. Aβ-spiked fresh human capillary whole blood (CPWB) specimens used to verify the accuracy were traceable to NIST standards with recoveries of 100.15± 1.2% and 98.6±1.1% and the imprecision results are 3.2% vs. 6.0% (n=18, n=15) for CA and DSCPO method, respectively. The results of the signal to noise ratio for both methods are about 12.

***Keywords*:** Nanobiomimetic Neural Memcapacitor; Voltage Sensor and Amperometric Sensor; Reagent-less.

INTRODUCTION

Amyloid-beta (Aβ) peptide accumulation and neurofibrillary tangle identified as major pathological biomarkers linked to Alzheimer's disease (AD) has been studied over decades. Besides significant progresses have been made, but lack of effective treatments and preventions addressed an urgent need for early diagnose and detection of Alzheimer's disease. It is estimated the global prevalence of dementia is about 24 million, and will double to 2040, leading to a costly burden disease to the society [1-3].

It would be more attractive to have a less invasive method to use than the CSF fluid method and to have an inexpensive method to use compared to a costly positron emission tomography with radiotracers. Therefore, plasma or human serum would be more desirable as specimens. Several road blocks have been hampered to reach the goals: the instability of Aβ in biological fluid [4-6], protein non-specific bounding caused high imprecision [4,7] and the time consuming procedures of the assay. The human biomarkers for Alzheimer's research are predominantly quantified using enzyme-linked immunosorbent assays (ELISAs) that are associated imprecision of CV% values reported in literature about 20-30% [4,7]. Calls for development of innovative tools and therapeutic approaches for better measuring preclinical and clinical biomarkers and treatment for AD is needed urgently [8-10]. Based on our experiences in development of nanostructured biomimetic sensors used for detection of toxins, blood glucose, cancers and neurotransmitters, such as acetylcholine (ACH) in biological fluid with selectivity, sensitivity and accuracy under the conditions of tracers-free, antibody-free and reagent-less [11-16], overcoming the challenges to developing nanostructured dual devices for precisely measuring preclinical Aβ in clinical useful range is encouraging to us. Providing even more useful information to clinicians and to patients is always beneficial.

Our biomimetic acetylcholinesterase (ACHE) membrane with an ACHE active site gorge deposited on a gold chip could be a best candidate to sense the presence of excess monomer Aβ, because ACHE dysregulation is well known to link to cancer, AD and other diseases [17-18]. However, direct measure Aβ, not ACH, in blood is a challenge, even though we used this "normal ACHE gorge" sensor to quantitatively detect ACHE in fM in amperometric mode [15] against a "mutated ACHE gorge" sensor, which was unable to sense ACH. Furthermore, we found the normal ACHE gorge sensor is able to serve as a memcapacitor type of memory device that clearly distinguishes conformational and neuronal circuitry change due to brain cancer cells' "bio-communicating" to the sensor [16]. Therefore, we hope the dual sensor would be able to sense the presence of Aβ in pM in order to lay a foundation for further study of the role of Aβ.

EXPERIMENTAL

Fabrication of the Nanostructure Self-Assembling Membrane (SAM) Gold Memristor Chips

The nanostructured Biomimetic "Normal Active ACHE Gorge" memcapacitor sensor with the flat bridged conformation/nanopore was freshly prepared and fabricated on gold chip. Polyethylene glycol diglycidyl ether (PEG), triacetyl-ß-cyclodextrin (T-CD), poly(4-vinylpyridine) (PVP) were purchased from Sigma. PVP was purified before use. The mono imidazolyl derivative dimethyl ß-cyclodextrin (mM-ß-DMCD) was generally synthesized according to the published procedures [19]. The procedures for mixture solution preparations of mM-ß-DMCD, T-CD, PEG, PVP and o-nitrophenyl acetate (o-NPA) and the gold chip membrane developments were followed according to the literature [20-21].

Characterization of the Membrane

The morphology of the AU/SAM was characterized using an Atomic Force Microscope (AFM) (model Multimode 8 ScanAsyst, Bruker, PA). Data Collected in PeakForce Tapping Mode. Probes used were ScanAsyst-air probes (Bruker, PA). The silicon tips on silicon nitride cantilevers have 2-5 nm radius. The nominal spring constant 0.4N/m was used. Figure 1 illustrates the 3D artificial neocortex-hippocampus memcapacitor design blocks as the neurons sensor. Figure 2 illustrates the 3D flat conformational bridge structure with "breathing nanopore" of the AFM images.

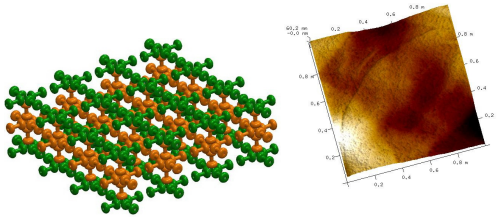

Fig. 1 (L) Illustrates the 3D memcapacitor blocks serve as the dual sensor. Greens represent conductive polymers; the oranges represent the inner "ACHE Gorge" in narrow cylinders connected through the neuronal terminals and dendrites as truncated donuts in compact flat metrics. Fig. 2 (R) 3D horizontal conformational bridge structure of the AFM images of the memcapacitor.

Overcome the Instability of Aβ

The CV method was used to identify the instability of Aβ in the aqueous media under the scan rate at 20 mV/s. After 0.1 mg/mL TCD was presented in the solution, the instability should be overcome, because β-cyclodextrin derivatives are well known stabilizers in industries [22].

Quantitation of Aβ

The CA Method. The CA method was used for quantitation of Aβ. $A\beta_{25-35}$ was purchased from Sigma. The data were acquired at room temperature under two-step fixed potentials in 8 concentration levels covering Aβ final concentrations ranging from 10^{-11}M to 10^{-7}M, with triplicates in DDH_2O with 0.1 mg/mL TCD and using an electrochemical work station (Epsilon, BASi, IN) with the companied software package. Origin 9.0 was used for all statistic data analysis and figure plotting.

The DSCPO Method. The characterization of the memcapacitor serving as a voltage sensor was conducted by the DSCPO method in ± 10 nA and 0.25 Hz in DDH_2O with 0.1 mg/mL TCD, with spiked Aβ final concentrations from 0.038 nM to 60.8 nM, and with triplicates for a calibration curve. The NIST SRM 965A human reference serum, with controlled blood glucose 70 mg/dL, spiked with Aβ having 4 levels from 3.8 to 417 nM with a single run at the same experimental conditions as in water media, and measurements without spiking Aβ were also taken for comparison.

Factors Affect on Sensor Performance

Peak duration time and Aβ concentrations were factors that affect on sensor's performance using the CA method. A healthy subject's fresh finger stick capillary whole blood (CPWB) specimens were collected, then immediately spiked Aβ in various concentrations in less than 4% water content to the blood volume without anticoagulant and without stabilizer. All measurements were in triplicates against controls at room temperature and finished in a half hour. Peak duration time had three levels: 4ms, 25 ms and 4s. The same factors were used for the voltage sensor under conditions of ± 10 nA and 0.25 Hz with data rate 1 kHz, 40, 250 Hz (both had data rate 50 kHz) for action potential peak or resting potential peak, respectively. The subject has gone through consent and was approved with the IRB.

Assessing Precision and Accuracy

Precision was evaluated by the two methods using fresh human CPWB specimens with triplicates at two levels of Aβ at 2.3 and 92 nM and three levels of frequencies at 0.25, 40 and 250 Hz in triplicates. Accuracy results were assessed by the "Point Accuracy" using signal means of the CPWB specimens against the calibration curves with the reference results that are traceable to NIST reference serum with the standard addition of the Aβ concentrations.

RESULTS AND DISCUSSIONS

Characterization of the Memristor/Memcapacitor

Literature reported electric synapse is one tenth of that of chemical synapse [23]. Fig. 3's i-V hysteresis curve was demonstrated with a switch point at the origin (0, 0). The frequency change affecting on the memristor/memcapacitor was depicted in Fig. 4 using NIST serum without Aβ. At low frequencies, the sensor has the highest *Direct Electron-relay Transfer* (DET) [10-12, 24] peak intensity than at high frequencies and all curves have hysteresis characters.

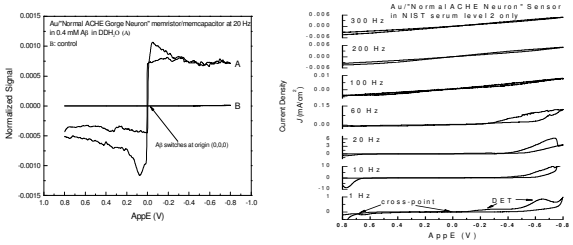

Fig 3 (L) Illustrates the hysteresis of the i-V curve of A in 400 µM Aβ in DDH_2O with a switch point at origin (0, 0, 0) against the control (B); Fig 4 (R) Depicts frequency affects on CV curves from 1 to 300 Hz in NIST serum without Aβ.

Overcome the Instability of Aβ

Instability of Aβ in various media has been reported in the literature [4-6], and our own experiments confirmed the instability in aqueous solution. The CV curves shown in Fig. 3 and Fig. 5 (L) illustrate the peaks were unstable in water. After 0.1 mg/mL TCD presences in the media, the CV curves are stabilized as shown in Fig. 6.

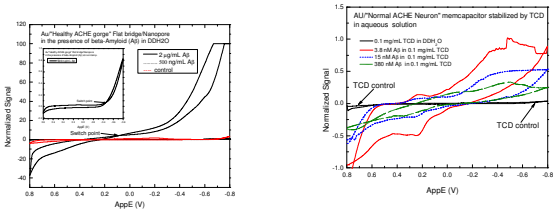

Fig. 5 (L) Illustrates the CV profiles without TCD. The control is in red; the insert is 380 nM Aβ; the solid black line is 1.52 µM Aβ. Fig. 6 depicts the i-V behaviors of the sensor in the stabilizer. Aβ at 0, 3.8, 15, 380 nM.

Quantitation of Aβ

The CA Method. Fig. 7 illustrates CA curve profiles in the presence of Aβ in aqueous solutions over the range of 0.037 to 151 nM Aβ. Fig. 8 illustrates the calibration curve with a linear regression equation Y= 0.59 +0.63X, r=0.998 (n=23), P<0.0001, Sy/x=1.96. The value of Detection of Limit (DOL) is $5.0x10^{-11}$M per cm^2 with a pooled relative standard deviation of 0.2% related to that at the mean concentration. Because this sensor is only 0.031 cm^2, hence, its DOL is 1.6 pM Aβ.

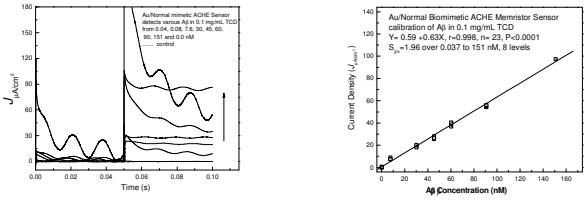

Fig. 7 (L) Illustrates CA curve profiles and Fig. 8 (R) shows the calibration plot of current density vs. Aβ concentrations.

The DSCPO Method. The magnitude of voltage change was the highest when without Aβ, as shown in the insert in Fig. 9. The calibration curve, as shown in Fig. 10, was inversely proportional to Aβ concentrations with a linear regression curve in water (in black) equation Y =1.48 - 0.018X, r = -0.992, $S_{y/x}$ =0.058, n=12, p<0.0001 over volumetric energy density from 0.41 to 1.50 µWHr/cm^3. The Detection of Limit (DOL) is $2.63x10^{-9}$M per cm^3 with a pooled relative standard deviation of 5% related to that at the mean concentration. Because this sensor is only $3.11x10^{-7}$ cm^3, hence, its DOL is $8.2x10^{-16}$M Aβ.

The Aβ calibration curve using NIST's reference human serum is shown in Fig. 10 in red and the experimental DSCPO curves profiles are shown in Fig. 11 covering clinically useful range between 3.8 to 471 nM Aβ. The linear regression equation of Y = 7.51 -0.014X, r = -0.995, Sy/x =0.36, N=4, p<0.005. The DOL value is $7.0x10^{-13}$M/cm^3.

Our results demonstrated Aβ is a strong inhibitor agent in blocking memory consolidating at Slow-Wave-Sleeping (SWS) at 0.25 Hz with the initial energy intensity decrease by 94% in 3.8 nM Aβ in serum. The energy signal without spiking Aβ is 8.5-fold higher in the serum than in the aqueous solution which indicates the serum is more suitable to the neuronal memcapacitor sensor without instability observed.

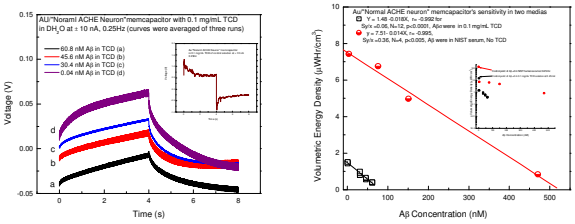

Fig. 9 (L) Depicts the DSCPO profiles in aqueous solution, and the curve with zero Aβ was in the insert. Fig. 10 (R) illustrates the calibration curves in NIST serum (Red), and in water (black).

The DSCPO profiles in the presence of Aβ in NIST serum samples were depicted in Fig. 11. The insert shows the curve without Aβ.

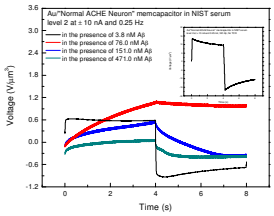

Fig. 11 Depicts DSCPO profiles of Aβ in NIST serum.

Factors Affect Sensors' Performance

Figure 12 revealed the high energy density values were associated with specific capacitance values between 1.2-2.2 F/cm^3 around zero Aβ compared with the negligible energy density at high Aβ level based on the calculations on the literature [25-26]. Fig. 13's map revealed the results obtained by a CA method using the same fresh human fresh CPWB specimens with the larger current density correlated with the highest Aβ concentration that located in the higher frequency at 250 Hz.

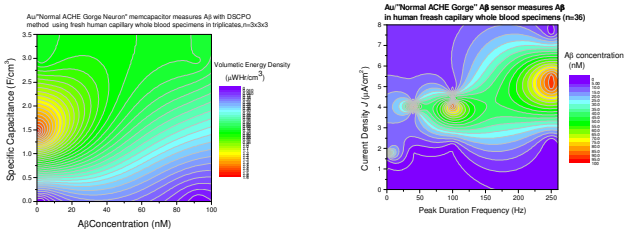

Fig. 12 (L) depicts the voltage sensor's factor map and Fig. 13 (R) depicts the CA sensor's factor map.

Assessing Precision and Accuracy

The imprecision was measured by the CPWB samples for the two sensors with the Pooled RSD of 3.2% (n=18) vs. 6.0% (n=15) over the studied ranges for the CA and the DSCPO method, respectively. The inaccuracy error was 0.1% with a recovery of 100.15± 1.2% for CA method after corrected metrics ratio. The average inaccuracy error obtained from the DSCPO method are 0.01% and 1.4% in water and in serum, respectively, that were traceable to the NIST's reference with 99.99±0.01% and 98.6±1.1% recovery.

The ratio of *Signal to Noise* (S/N) values accessed by the CA method and the DSCPO methods were calculated based on the conventional teaching [27]. The results have *S/N* values of 11.63 vs. 12.5 for the CA and DSCPO method, respectively.

CONCLUSION

The dual sensors detected sub pM Aβ with near 100% recoveries and 3-6% imprecision under antibody-free and tracer-free conditions were demonstrated. The technology may find wide applications for early monitoring of Alzheimer's disease.

REFERENCES

[1]. Reitz C, Brayne C and Mayeux R, *Epidemiology of Alzheimer disease,* Nature Reviews Neurology 7, 137-152, 2011.

[2]. John E. Morleya JE and Farr SA, Biochemical Pharmacology, 88(4), 479-485, 2014.

[3]. Jia Q, Deng Y, and Qing H, BioMed Research International Article ID 837157, 22 pages, 2014.

[4]. Toledo JB, Shaw LM and Trojanowski JQ, Alzheimer's Research & Therapy **5,** 8, 2013.

[5]**.** Lachno DR, Emerson JK, Vanderstichele H, et al, J Alzheimers Dis 32, 905-918, 2012.

[6]. Bibl M, Welge V, Esselmann H, Wiltfang J, Electrophoresis 33,445-450, 2012.

[7]. Esparza TJ, Zhao H, Cirrito JR, Cairns NJ et al., Ann Neurol,73(1), 104–119, 2013.

[8]. Fiandaca MS, Mapstone ME, Cheema AK, Federoff HJ, Alzheimer's & Dementia, 10, S196-S212, 2014.

[9]. Zlokovic BV, Neuron, 57(2),178-201, 2008.

[10].Chen ET, Duh SH, Ngatchou C, Thornton JT, and Kissinger PT, Nanotech (3),*101-104,* 2011**.**

[11].Chen ET. US Patent 6,582.583, June 24, 2003.

[12].Chen ET, US Patent 8,083,926, December 27, 2011.

[13].Chen ET, Thornton JT, Ngatchou C, Duh SH and Kissinger PT, NSTi-Nanotech (3), 115-118, 2013.

[14].Chen ET, Thornton JT, Ngatchou C, Duh SH and Kissinger PT, NSTI- Nanotech (2), 107-110, 2013**.**

[15]. Chen ET, Thornton J, Ngatchou C and Duh S-H. , NSTi-Nanotech, 2, 169-172, 2014.

[16].Chen ET, Thornton J and Mulchi Jr C. Sensors & Transducers, 183(12), 72-83, 2014.

[17].Nordberg A, Rinne JO, Kadir A and Långström B, Nature Reviews, 6, 78-87, 2010,

[18].Yan JJ, Cho A-Y, Kim H-S, Kim K-L, Jung J-S, British J of Pharmacology 133(1). 89–96, 2001

[19].Chen ET and Pardue HL, *Anal Chem,* 5, 2563-7, 1993.

[20].Chen ET, Thornton JT, Ngatchou C, Duh SH and Kissinger PT, NSTi- NanoTech (2), 107-110, 2013.

[21].Chen ET, Thornton JT, Ngatchou C, Duh SH, NSTi-Nanotech, 2, 200-203, 2014.

[22].Szejtli, *Cyclodextrin and Their Industrial Uses,* Editions de Sant´e, Paris, 1987.

[23].Buzsáki G et al., Nature Reviews 13, 407-420, 2012.

[24].Chen ET, *Nanobiomimetic sensing and energy storage* in the first volume of the book series of *Dekker Encyclopedia of Nanoscience and Nanotechnology* edited by Lyshevski SE, CRC Press*,* 2013.

[25].Hu L, Choi JW, Yang Y, Jeong S, Mantia FL, Cui L-F and Cui Y, PNAS 106 (51), 21490-21494, 2009.

[26].Thornton J, Christelle C and Chen ET, NSTi-Nanotech (2), 672-675, 2013.

[27].Skoog DA and Leary JJ, *Principles of Instrumental Analysis,* Fourth Edition, Saunders College Publishing, 1992.